Published by :
http://www.ijert.org

International Journal of Engineering Research & Technology (IJERT)
ISSN: 2278-0181
Vol. 12 Issue 02, February-2023

Computational Simulation Study on Slab Steel Continuous Casting Fluid Dynamics to Avoid Mold Flux Entrapment

Javier Sola, Guillermo Díaz, Elena Brandaleze
Metallurgy Department, DEYTEMA Centre
Universidad Tecnológica Nacional-Facultad Regional San Nicolás,
San Nicolás, Argentina

***Abstract*— The continuous casting process constitutes one of the most important ways for the steel production in the world. The steel product quality requirements are high and the industry impulse different research with the purpose to avoid product defects and operation problems. The computational simulation integrated with experimental assays constitute a good alternative to deep the knowledge of different fluid phenomena that are present during the initial stage of steel solidification in the continuous casting mold at processing conditions, that could cause quality defects. In this paper, the mold flux entrapment defect susceptibility in relation with casting speed and mold width variation was considered. To carry out the study different computational tools were applied to evaluate the fluid dynamics and the thermodynamic evolution of the complex system in the mold. The results included steel and mold flux physical properties values estimations. The information obtained allows to predict the operation conditions that could increase the mold flux entrapment risk during HSLA steel continuous casting process for the industrial selected conditions and it is considered relevant for steel slabs processing in the steelmaking industry.**

Keywords—Computational simulation, mold powder entrapment, steel continuous casting

I. INTRODUCTION

The continuous casting process (CC) has been widely developed as one of the most important production processes in the steelmaking industry. Currently 97% of steel products are produced by CC and in the slabs production at large scale is one of the most used industrial methods for steel solidification. During the operation, the molten steel is poured from a ladle into a tundish. Then liquid steel flows through a submerged entry nozzle (SEN) into a water-cooled copper mold. During steel solidification, in the continuous casting mold, it is necessary to removes heat from the liquid steel up to temperatures below the melting point because of the latent heat (exothermic enthalpy) release required, to induce the liquid to solid transformation. Against the water-cooled copper mold walls, a steel solid shell is formed and contains the molten steel. At this stage, heat extraction and lubrication between the steel shell and the mold constitute relevant points of control to avoid operation problems or steel product quality defects. Mold flux entrapment constitutes an important defect that could be generated during steel continuous casting, and it is relevant to understand deeply the origin mechanisms involved.

During the initial stage of solidification, a combination of different phenomena occurs: (1) gas emissions, (2) mold flux emulsification, (3) non-metallic inclusions removal, (4) homogenization of molten steel, among others. All of them involve a very complex multi-phase physicochemical reactions and specific fluid dynamic characteristics [1].

In order to improve steel slab quality, it is relevant to carry out an integrated study considering the variables of the CC process and involve different critic zones of the upper part of the mold: mold flux-metal interface, the meniscus zone, impact of jet flow zone and the steel shell. All of them, are relevant during the initial stage of the steel solidification.

Many researchers were studied the mold flux entrapment problem, Mills in [2], informs nine possible origin mechanisms and concluded that this type of quality problem is a result of: (a) slag crawling (aided by pressure differences across the SEN), (b) Karman vortices, (c) Kelvin–Helmholtz instabilities, (d) SEN immersion depth and (e) upward flows. To avoid the problem, it is possible to consider: (a) the casting speed decrease, (b) interfacial tension increase (c) slag viscosity increases and improving thermal insulation in the mold flux bed (particularly to avoid hook formation and meniscus balding). Low mold level variations are unlikely to cause mold flux entrapment. However, the turbulence presence in the surface increases the defect risk. To understand the problem, it is relevant to dispose information on fluid dynamics through process simulation. The entrapment is mainly affected by the metal flow velocity and the flow pattern (single and double roll), the physical properties behaviour of the mold flux and of the liquid steel, in correlation with operation variables [3, 4]. Steel chemical composition determines the behaviour at the meniscus zone. It is relevant to dispose the values of steel liquidus temperature (T_L), viscosity (η) and surface tension (γ). In addition, the specific phase diagrams, to predict the phases evolution of the steel and the mold flux, constitute good information to consider. In this sense, the solidification path analysis under Scheil cooling (paraequillibrium conditions) provides very useful information to understand the initial stages of solidification, including phases evolution [5].

As was previously mentioned, at the initial solidification moments, stable mold level conditions are important also to achieve the formation of a steel shell that contains inside the liquid steel. The shell must be thick enough to withstand the ferrostatic pressure of the so-called liquid vein contained inside the product, which continues cooling towards the

International Journal of Engineering Research & Technology (IJERT)
ISSN: 2278-0181
Vol. 12 Issue 02, February-2023

bottom of the mold. Then, through extractor rollers and cooling spike systems, the product solidification and extraction continue. By this way, semi-finished products are obtained such as slabs (which after hot and cold rolling processes, are transformed into steel sheets).

In this paper the analysis of combined effects such as width change together with the variation of the casting speed in the mold, for liquid steel-mold flux system, is approached with an integrated point of view to evaluate the impact on mold flux entrapment problem. This defect is affected by the instability and asymmetry of the fluid flows into the mold that affects steel product solidification. The turbulent flow in the mold level influences transport and entrapment (of mold powder, inclusions and bubbles), the fluctuation and shape of flux-metal interface, the dissipation of superheat, the entrainment of mold flux at the top surface and the growth of solidified shell. The transient asymmetric flow is a common fluid flow pattern in the continuous casting mold. The turbulence of molten steel inside the liquid pool is calculated in this study using the K-Ω SST model during 90 s, to develop the required flow and then other model with LES (Large Eddy Simulation) is used to achieve a higher time precision. The computational modeling was carried out applying ANSYS Fluent. To increase the knowledge on the mold flux entrapment phenomenon that occurs at the (mold flux-liquid steel) interface, for different industrial operation conditions, Computational Fluid Dynamics (CFD) simulations were carried out at the meniscus zone, considering: different casting speeds, different mold widths and the same submerged nozzle depth.

The mold flux constitutes a very important input in the steel continuous casting. It consists in a complex oxides system, minerals, and carbonaceous materials. It is added by the upper part of the mold, manually or automatically. The flux covers the liquid metal and surround the submerged nozzle. These fluxes fulfill a series of critical functions for the mentioned process [2]: controls the heat transfer towards the mold and the atmosphere, protects the liquid steel from re-oxidation by contact with air, provides lubrication between the solidified shell and the mold wall and picks up inclusions at the flux-metal interface. Lubrication is directly related to the physical properties of the mold flux selected for each steel grade, such as its viscosity and fluidity [2, 3].

In this study, the results obtained by FLUENT simulation involved steel and mold flux properties values. The steel T_L was determined by Irving et al. model [6] and was correlated with results of Scheil cooling predictions obtained using Fact Sage 8.1. The value of the steel viscosity considered is 0.006 to 0.007 Pa.s) reported in [7].

The mold flux characterization includes different aspects such as: melting critical temperatures determination, viscosity and surface tension values (at interest conditions) and the crystallization tendency during cooling. In this paper, the physical properties were determined by experimental tests and thermodynamic simulations (applying Fact Sage 8.1) [8, 9].

II. METHODOLOGY

The HSLA steel selected for this study is a B-Ti steel with high boron content (≅ 42 ppm B and 32 ppm of N). These steel slabs are used in the automotive industry, to produce special machine components for demanding applications: forged thick steel plates, rods, blocks, pulleys, etc.). These applications require very high qualities slabs, without defects, free of shrinkage, porosity, segregation, or cracks. Through numerical modelling, the steel liquid behaviour during mold filling and mold flux entrapment phenomenon can be predicted. The steel chemical composition is observed in Table I. The operation parameters selected for the study considers a casting temperature T_c=1530ºC and three casting speeds: c_s=1 m/min, c_s=1.5 m/min and c_s=1.8 m/min. The casting mold width used are: 900 mm and 1600 mm. For both cases the same nozzle depth was considered (100 mm). The chemical composition of the mold powder used is detailed in Table II.

The mold flux melting behavior and the evolution of the contact angle values (θ) (in relation with temperature) were determined by means of a hot plate microscopy (HSM) assay. The test provides four critical temperatures values: initial temperature (T_i), softening temperature (T_s), hemisphere temperature (T_h) and fluidity temperature (T_f). The contact angle values (θ) are used to calculate the surface tension of the mold flux through (1), at the temperature of interest. This expression corresponds to a calculus model developed based on the Jurin modified law, where: γ is the surface tension, h is the drop high, ρ is the molten flux density, g is the gravity acceleration and θ the contact angle.

$$\gamma = h^2 \rho g / 2(1-\cos\theta) \quad (1)$$

The mold flux viscosity evolution associated with temperature was predicted by Fact Sage 8.1, applying the viscosity modulus [9]. The physical properties results obtained are used to complete the study of the system steel-mold flux interface at casting operation conditions and constitute the input values for FLUENT simulations. In addition, to understand the mold powder crystallization tendency during cooling, a Scheil cooling calculus was carried out (by Fact Sage 8.1), considering the temperature range of interests.

The crystallization tendency of the mold powder was also experimentally evaluated by a quenching test pouring the molten flux on a steel plate and then evaluating the samples by light microscopy applying an Olympus GX 51 instrument with image analysis system Material Plus.

TABLE I. HSLA STEEL CHEMICAL COMPOSITION

Element	% Wt.
C	0.30
Mn	1.46
Si	0.17
Ti	0.035
P	0.015
S	0.0039
B	0.0042
N	0.0032

International Journal of Engineering Research & Technology (IJERT)
ISSN: 2278-0181
Vol. 12 Issue 02, February-2023

TABLE II. MOLD POWDER CHEMICAL COMPOSITION

Compound	% Wt.
SiO_2	33.0
CaO	29.0
MgO	1.28
Al_2O_3	4.30
$Na_2O+ K_2O$	9.69
Fe_2O_3	0.57
MnO	0.10
F	9.11
TiO_2	0.05

It is relevant to comment that the multiphase CFD model used, considers a free surface and at the same time high resolution of vortices, for this reason the computational requirements could be unfeasible. Fig 1 detailed a 2D model that was selected for this study, with the domain and boundary conditions.

To define the domain, two geometries were adopted: a) one representing a mold width of 900 mm and b) the other with a mold width of 1600 mm. In both cases the submersion depth of the (SEN) considered was 100 mm.

For the inlet speed, three values are adopted with the purpose of evaluate the impact in the fluid dynamic pattern: 1 m/min, 1.5 m/min and 1.8 m/min. The atmospheric pressure on the free surface was set at P=101325 Pa.

The outlet condition considered is the total pressure (static pressure + dynamic pressure) in the mold. The mold wall boundary condition was adopted as shear condition without slip.

For meshing, the predominant square type elements were adopted. Fig. 2, shows the refined mesh used in the interest areas such as the air/powder and steel-flux interfaces, to achieve a more precision on the dynamic flows in these areas.

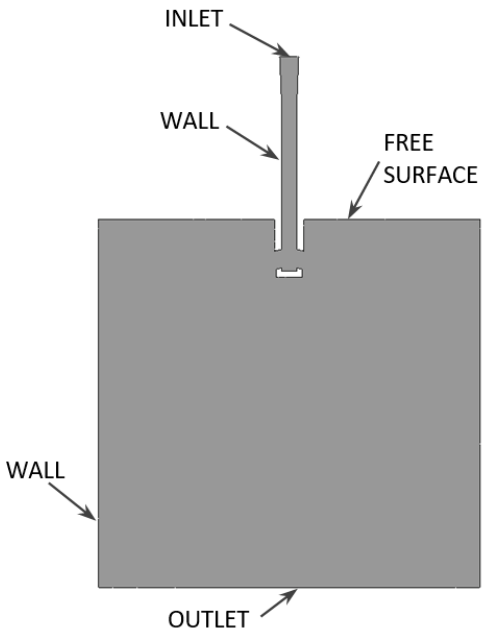

Fig. 1. Domain and boundary conditions selected for the computational simulation.

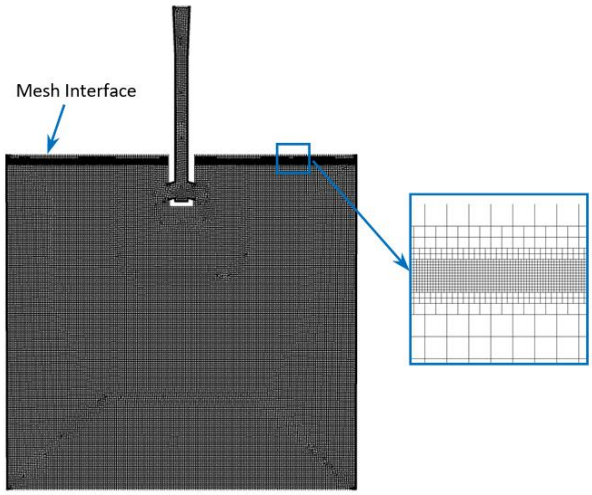

Fig. 2. Domain mesh used for the simulation.

The main equation of computational fluid dynamics (CFD) is known as the Navier-Stokes equations, and which are considered constitutive relations or equations of state. The Navier-Stokes equations consist of mass, momentum, energy, etc. conservation equations [10, 11].

In this paper, for the steel – mould flux – air system simulation, the Volume of Fluid (VOF) model was used based on previous research informed in [12]. It is relevant to comment that this model, relies on not all fluids in the domain are interpenetrating. In addition, in each control cell the volume fraction of the phases sums to unity. A powerful interface treatment condition was used. To simulate turbulence, the two stages selected are described: a) a run with the K-Ω SST model for 90 seconds used to develop an approximate flux, b) a run with LES model (Large Eddy Simulation) to complete the simulation [4]. The LES model can capture details of the transient motion, accurately. This model also solves the larger scale vortices while the smaller scale ones are calculated by statistical models. The phases were established in an air layer of 300 mm and the mould flux layer of 3 mm, above the steel uniformly distributed and below the free surface. It is relevant to mentioned that a SIMPLE algorithm is used to solve the coupling of the pressure and speed fields. Fig. 3 shows the result obtained. The understanding of the flow pattern in the molten steel pool is necessary to improves the casting conditions and avoid the quality defects. The avoidance of flux entrainment and non-metallic inclusions in the final product is the major goal in continuous casting. The flow pattern at casting conditions, directly affects flux entrapment defect tendency. Many defects in steel slabs generated in the continuous casting process are caused by undesirable surface flow or severe fluctuations at the interface between molten steel and mold flux. The impact of the casting speed variations together with the mold width changes used for the B-Ti steel slabs casting, are considered important points of study to decrease the products dismiss in the steel plant.

The impact of the casting speed variations together with the mold width changes used for the B-Ti steel slabs casting,

International Journal of Engineering Research & Technology (IJERT)
ISSN: 2278-0181
Vol. 12 Issue 02, February-2023

are considered important points of study to decrease the products dismiss in the steel plant.

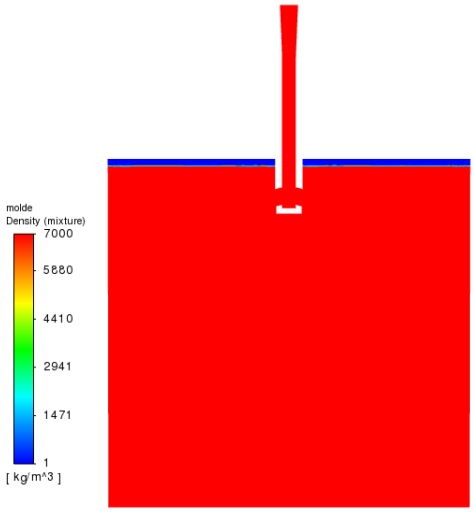

Fig. 3. Diagram of liquid densities.

III. STEEL AND MOLD FLUX BEHAVIOR AT CASTING CONDITIONS

The High Strength Low Alloy steels (HSLA) are increasingly used in the automotive industry because of their good combination of ductility and strength. The steel selected for this study contains boron which can provide a hardenability effect equivalent to adding 0.5% of other elements such as Mn, Cr and Mo, with a good mechanical behaviour and low cost [12]. However, in order to produce car body parts by hot stamping process a very high quality of the semi-product is required. This means to obtain slabs by continuous casting free of defects or cracks. For this reason, it is necessary to improve the production technology of HSLA slabs, selecting the best casting temperature, a good flow pattern, an adequate turbulence at the mold level, to optimize the regime of mold filling and minimize defects [13]. With this purpose it is necessary to dispose information on the steel liquidus temperature T_L, viscosity values η and phases evolution of the steel during cooling. Applying the Irving model [6], on the base of the steel chemical composition, the liquidus temperature value was calculated and the value resulted T_L= 1502ºC. Considering that the continuous casting temperature in the process is (T_c=1530ºC), it is possible to note that the liquid steel during the casting process is at ~28 °C above the liquidus temperature. Fig. 4 shows the cooling predictions carried out by thermodynamic simulation applying Scheil-Gulliver method for the HSLA steel, using Fact Sage 8.1. The critical temperatures and the main phases evolution were obtained. In addition, the T_L value estimated by Irving model was also corroborated. The steel evolution during cooling, indicates the nucleation of a low quantity of delta ferrite (δ) phase, at T ~ 1500°C. This phase is constituted by a solid solution of carbon in iron (BCC). Then, the continuous cooling promotes the transformation of delta ferrite phase to austenite phase ($\delta \rightarrow \gamma$). Austenite ($\gamma$) is the solid solution constituted by carbon in iron (FCC). Finally, at T=725°C, a new phase transformation occurs from austenite (γ) to alpha ferrite (α) phase. The $\gamma \rightarrow \alpha$ phase transformation involves that (γ) solid solution (constituted by carbon in iron FCC) is transformed to α solid solution (of carbon in iron BCC).

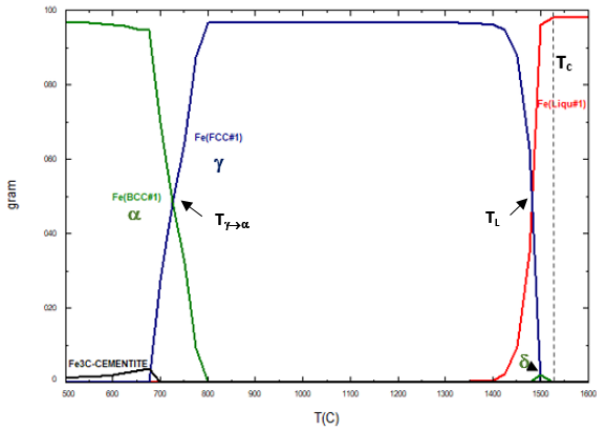

Fig. 4. HSLA steel critical temperatures and phases evolution determined by Scheil cooling simulation by FactSage.

At lower temperatures than 700°C, a low quantity of cementite (Fe_3C) formation is predicted. According with the experimental values determined in [7] for similar boron steels, the viscosity values at 1530°C are between 0.0271 to 0.0298 Pa.s.

The mold flux input in the continuous casting process is the other relevant factor to be consider in this study. The characterization of the material provides: a) basicity index (IB), b) fluidity between 1400°C to 1200°C (measured by inclined plane), c) viscosity at the same temperatures range (calculated by FactSage), d) the melting behaviour (obtained by HSM tests) and e) crystallization tendency carried out by light microscopy on quenched samples since 1300°C. The physical and chemical properties of the mold powder are detailed in Table III.

The basicity index value (IB=0.88) agrees with the common mold flux used for this steel grade processing. The physical properties shows that fluidity at temperatures between 1400ºC and 1200ºC decreases ~29.5%, this result is consistent with the viscosity and surface tension increase at the same temperature range. The critical temperatures obtained through HSM test, corroborates that the mold flux is fully melted when steel solidification starts. The correlation of all the physical properties results allow to think that the mold flux at continuous casting solidification conditions provides good physical properties to guaranty the required lubrication [3].

TABLE III. MOLD POWDER PHYSICAL AND CHEMICAL PROPERTIES.

Property	Condition	Value
IB		0.88
Fluidity Layer length (mm)	T=1400°C	248±4
	T=1300°C	216±5
	T=1200°C	175±2
Viscosity η (Pa.s)	T=1400°C	0.152
	T=1300°C	0.428
	T=1200°C	1.606
Surface Tension	T=1400°C	164.2
	T=1300°C	168.6

International Journal of Engineering Research & Technology (IJERT)
ISSN: 2278-0181
Vol. 12 Issue 02, February-2023

γ (mN/m)	T=1200°C	172.9
T_{break} (°C)		1107
Melting behaviour (°C)	T_I	20
	$T_{softening}$	1061
	$T_{hemisphere}$	1074
	$T_{fluidity}$	1118

The crystallization tendency is determined through the quenched test and quantified by light microscopy measurements. The methodology constitutes a comparative procedure usually used in the mold flux control. During the test, mold flux is melted and poured over a steel plate inclined 10°. Then samples are extracted from the layers are prepared for microstructural observation. Fig 5 shows the crystalline layer observed in the surface of the quenched sample and applying longitudinal measurements by the image analysis system the layer thickness, was measured.

In this material the measurements showed that the crystallization tendency is low (incipient) because the crystalline layer constituted by dendritic crystals developed in the surface of the sample during the quench test, presented a thin thickness ≤ 50 μm. In addition, no crystals were identified in the inner glassy zone of the sample.

The phases evolution (liquid and crystalline) during cooling of the mold powder was also predicted applying Scheil cooling simulation applying Fact Sage 8.1, including back diffusion predictions.

The results obtained by the thermodynamic simulation were consistent with the T_{break} value, determined by theoretical calculus according with [2]. At temperatures T > T_{break} the mold powder is fully liquid. However, at T_{break} proximity, phases crystallization starts and the liquid phase mass decrease. In consequence, the physical properties (viscosity, fluidity and surface tension) behaviour starts to change.

It is relevant to consider that this mold powder is characterized by a low T_{break} with the purpose of provide the adequate heat extraction at the meniscus level. In addition, the important proportion of liquid phase in the mold powder guarantee an important heat extraction during the initial solidification stage.

Fig. 6 shows that three main crystalline phases are generated during mold powder cooling, in the continuous casting. At high temperature conditions (~ 1125ºC), the liquid phase present in the melted mold powder is > 80% promoting an important radiation heat extraction component at the initial solidification of the HSLA steel.

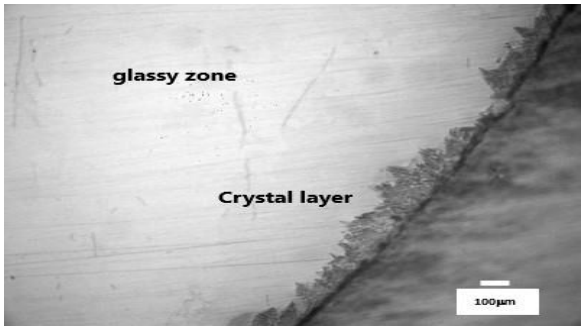

Fig. 5. Mold flux crystalline layer developed in the sample surface under quenched test.

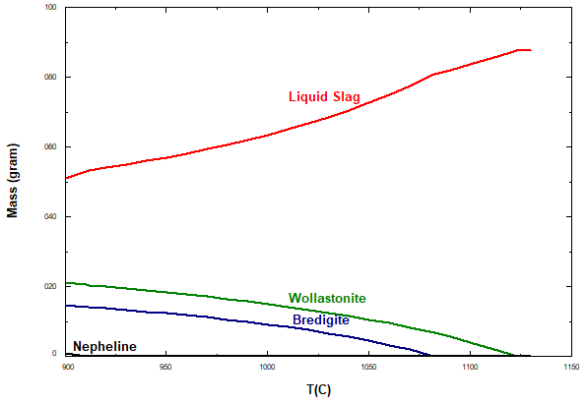

Fig. 6. Mold flux phases evolution during cooling predicted by Schail cooling applying Fact Sage.

The first and main crystalline phase which starts to precipitate in the system is Wollastonite (β-$CaSiO_3$) at T~ 1122°C. The second phase predicted is (Bredigite, $Ca_7Mg(SiO_4)_4$) and their nucleation and precipitation process starts at T ~ 1082°C. Finally, a low quantity of Nepheline $NaAlSiO_4$ precipitates at temperatures around 911°C. The mold flux crystallization tendency during cooling affects the resistance of the Cu/slag interface and reduces the heat flux in the mold. The combination of crystalline phases provides the adequate steel heat extraction in the continuous casting mold.

IV. MOLD POWDER ENTRAPMENT SIMULTAION

The interfacial tension present in the system mold flux-steel (γ_{ms}) influences: a) mold flux entrapment susceptibility, b) the meniscus shape, c) the characteristics of the oscillation marks among other aspects. High interfacial tension (γ_{ms}) minimize the entrapment risk. However, the higher meniscus temperature is, the lower surface tension (γ_{ms}) value is. For this reason, during casting the risk of mold flux entrapment increases with higher meniscus temperature and in consequence low (γ_{ms}). In this study the simulation considered the value γ_{ms}=164.2 mN/m, estimated on the base of the contact angle measurements carried out by HSM experimental test at 1400°C. The simulation result shows that in the mold flux entrapment three dominant forces are present, two of them are stabilizing forces: a) Flotation force (F_f) and b) Surface Tension force (F_γ) which depend on the steel and mold powder physical properties. The third force is the inertial force, that constitutes a destabilizing force which depends on the flow of the phases present in the interface (steel-mold powder). This force favors the trapping phenomenon. The inertial force is determined by the speed difference between one side and the other respect to the mix layer together with their thickness. They are caused by the shear phenomenon present in the interface. In Fig.7, the phases present in the system and different forces are visualized.

In addition, at both sides of the mix layer a speed gradient is observed. The F_f force is promoted by the density differences between the steel and the mold powder. The greater the density gradient is, the more stable the interface becomes, for this reason they are considered stabilizing forces. In the steel-mold flux interface, the molten flux forms a film

International Journal of Engineering Research & Technology (IJERT)
ISSN: 2278-0181
Vol. 12 Issue 02, February-2023

with a surface tension due to the molecular attraction from internal molecules present in the liquid phase volume.

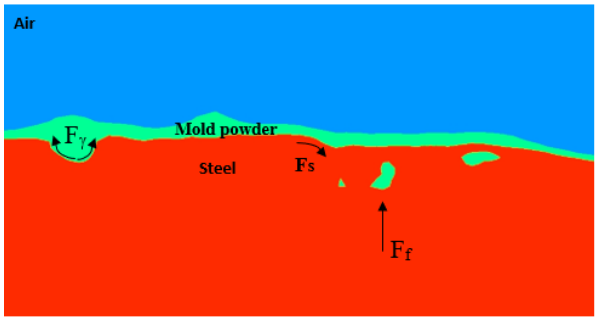

Fig. 7. Phases and forces present in the steel-mold flux system.

The force required for the film generation is known as a surface tension force (Fγ) and it acts as a stabilizing force during each external perturbance in the interface. Fig.8 (a) and (b) present the simulation results obtained considering a casting speed of 1 m/min for both mold widths (900 mm and 1600 mm). It is possible to note that the interface not present relevant surface perturbations and in consequence it is possible to think that the susceptibility to mold flux entrapment is negligible and not affected by the mold width at this speed casting. However, Fig.9 (a) and (b) show diagrams of speed vectors and density which results of the simulations carried out at 1.5 m/min for both mold widths. In this case a considerable surface perturbation appears, and the interface behavior indicates that the mold flux entrapment susceptibility is possible. In addition, in the diagram that corresponds to mold width 900 mm show that the jet impact on the mold wall induces a different flow pattern respect to the observed for the width 1600 mm, at the same casting speed condition. Two large recirculation above and below the fluid jet indicating a double roll is observed for the mold of 900 mm, meanwhile for the width 1600 mm a single roll fluid pattern is predicted. In both cases the surface perturbation increases, and the velocity vector values present considerable variations between both cases. The critical zone for the mold flux entrapment possibility is observed near the SEN.

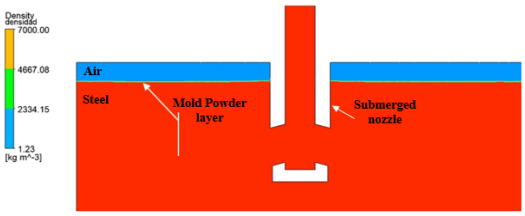

(a)

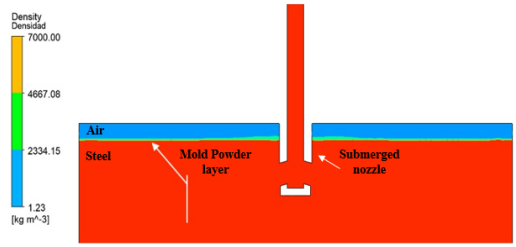

(b)

Fig. 8. Density diagram obtained for the casting speed 1m/min. (a) mold widths 900 mm and (b) mold widths 1600 mm.

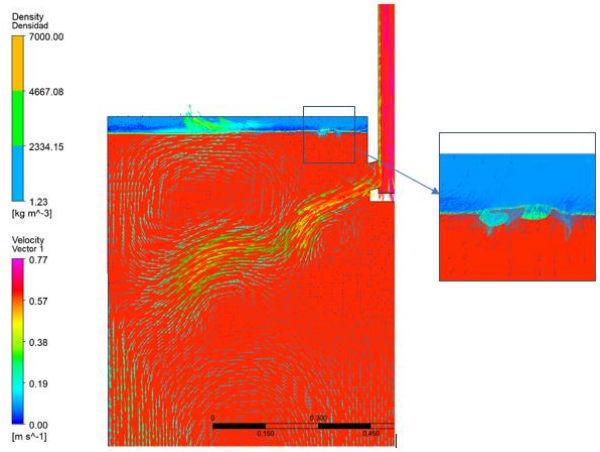

(a)

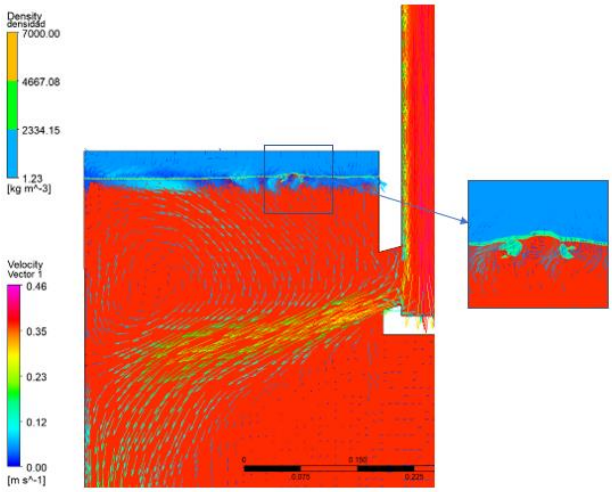

(b)

Fig. 9. Diagram of speed verctors and density obtained for the casting speed 1.5 m/min. (a) mold widths 900 mm and (b) mold widths 1600 mm.

It is relevant to note that both figures present amplified images of the critical zone to show in more detail the surface perturbance predicted near the SEN. Fig. 10 (a) and (b), present the simulations at higher casting speed (1.8 m/min). It is visualized that the mold flux entrapment defect risk increases because of the interface perturbance intensification. The flow pattern between both mold widths also is different respect the previous casting speed (1.5 m/min) condition analyzed. At the high casting speed, the double roll is predicted for the mold width 1600 mm meanwhile for 900 mm a single roll is observed. The results also show that at casting speeds (1.5 m/min and 1.8 m/min) for both mold widths, the meniscus level experiences a hump near the mold wall and a considerable surface perturbation that increment the mold powder entrapment risk. However, this phenomenon is considerable intensified at 1.8 m/min because of the recirculating flow in the upper zone of the mold. It is relevant to consider that severe fluctuations in meniscus level will disturb the slag infiltration between the steel shell and the mold causing also heat flux variations, especially in the area at

International Journal of Engineering Research & Technology (IJERT)
ISSN: 2278-0181
Vol. 12 Issue 02, February-2023

20−60 mm from the mold corner, adding risks of other quality product defects.

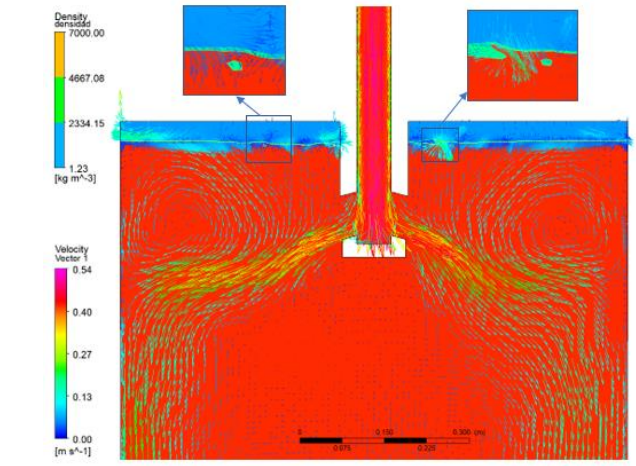

(a)

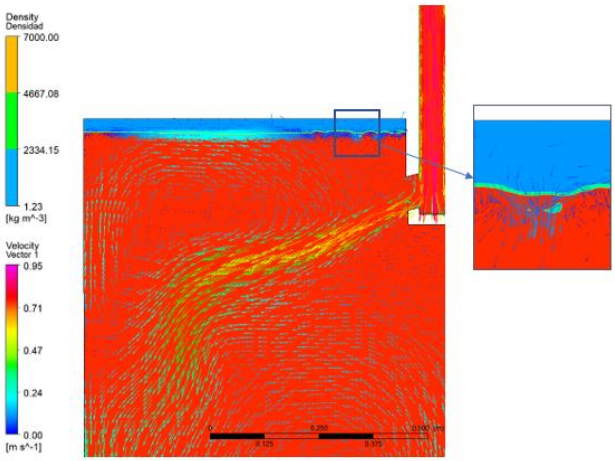

(b)

Fig. 10. Diagram of speed verctors and density obtained for the casting speed 1.8 m/min. (a) mold width 900 mm and (b) mold width 1600 mm.

In agreement with [14], the casting speed increase produces a recirculating zone expansion, that is, deeper impacting depth and higher liquid level perturbations, see Fig 9 and 10. The mold surface perturbation results in mold powder film thickness variations. When near the mold wall the liquid mold powder layer becomes very thin, the infiltration is turned complex and could cause sticking problems. In this case of study, it is possible to consider that the mold flux considered (at meniscus temperature) presents a low viscosity ($\eta \leq 0.152$ Pa. s) and in consequence has a higher fluidity, and could promotes the entrapment probability. Nevertheless, the physical properties requirements of the mold powders in the continuous casting process involves to know: viscosity and surface tension γ_{ms}, at processing temperature combined with a low crystallization tendency, to guarantee the mold powder infiltration and lubrication during the initial stages of casting of this steel grade. This is considered a compromise condition. This physical behaviour is enhanced with the mold level temperature rise at high casting speeds. High casting speeds also results in a thinnest mold powder layer infiltration, changing the heat extraction during the steel solidification. It is relevant to achieve a homogeneous velocity distribution and of the flow pattern in the inlet region of the mold (in the casting direction) and to guarantee the heat transfer to obtain the uniform growth of the shell in the transversal direction of the product [15]. The fluid flow pattern and temperature variation in the solidification zone play an important role in achieving an homogeneous chemical composition in the product structure [16]. To evaluate deeply the nature of steel-mold flux interface, the interfacial acceleration values predicted by the simulation for both mold widths (900 mm and 1600 mm) were analyzed in the zone between the nozzle and the mold wall for each casting speed (1 m/min, 1.5 m/min and 1.8 m/min). Fig. 11 (a) and (b) show the acceleration values evolution of the component's "x" and "y". For the mold width 900 mm, the acceleration values, for both acceleration component direction (x and y), indicate a considerable interface perturbation in both cases and the effect increases with for major casting speed. It is noticeable that for this width the interface perturbation is more intense in the zone near the SEN (from x=0 to x~0.25 m), mainly at the right side of the mold. At the simulation time considered for the analysis, the acceleration component y= -0.35 m/s2, represents the major negative value (at x= 0.10 m), that could be considered as a possible localized mold powder drag tendency risk to the steel. The phenomenon was clearly observed for the casting speed 1.8 m/min. The comparison of the results obtained for the acceleration components, for both mold widths at the same casting conditions (1.8 m/min), indicate that the susceptibility of mold flux entrapment at this casting speed, is possible in both mold width cases. The strongest acceleration component which affects the interface perturbation and promotes the entrapment tendency are different between both cases. For the mold width 900 mm results the component "x" and for the mold width 1600 mm the component "y". This variation is probably produced by the flow pattern differences. Fig. 12 (a) and (b) show the acceleration values (in x and y) considering the same time and casting speed for a mold width 1600 mm. It is possible to compare the impact of the widths differences on the mold powder drag forces.

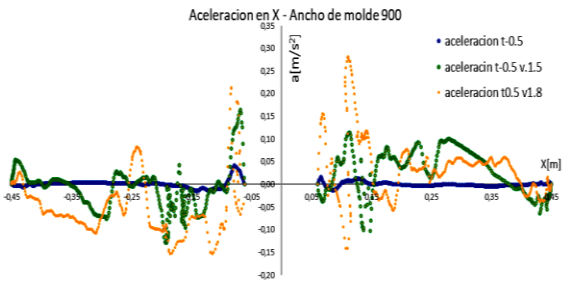

(a)

International Journal of Engineering Research & Technology (IJERT)
ISSN: 2278-0181
Vol. 12 Issue 02, February-2023

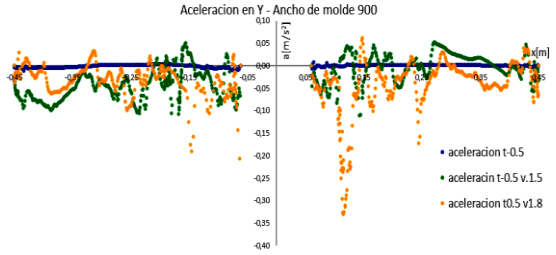

(b)

Fig. 11. Acceleration values predicted for the mold width 900 mm. (a) "x" direction and (b) "y" direction.

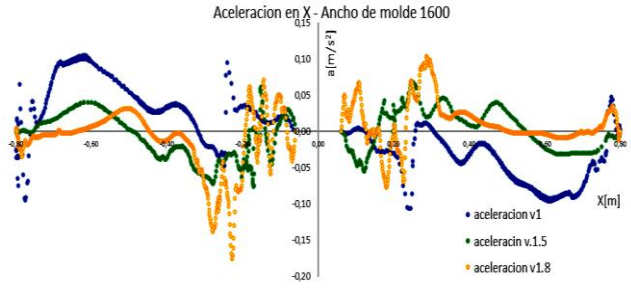

(a)

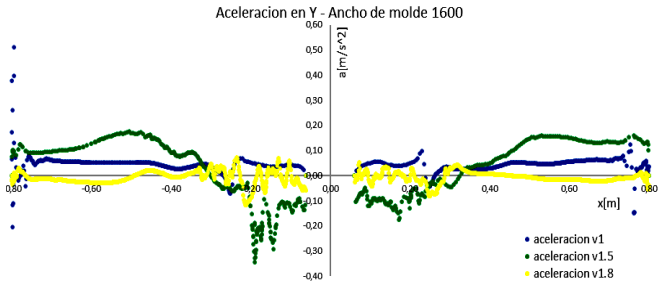

(b)

Fig 12. Acceleration values predicted for the mold width 1600 mm. (a) "x" direction and (b) "y" direction.

For the mold width 1600 mm, the interface perturbation is mainly affected by the acceleration component in "x" direction at different processing speeds. In addition, this perturbation is more intensive at the left mold side and the major negative acceleration value identified is -0.18 m/s^2 for a distance x = - 0.21 m (respect the nozzle). In this case, the acceleration component "y" values, presents the lowest interface perturbation.

The study allows to consider that for both mold widths the casting speed 1.8 m/min is critic, and the mold powder entrapment is possible. In addition, it was possible to visualized that the strongest acceleration component which affect the interface perturbation and promotes the entrapment tendency are the acceleration "x" component for the mold widths 900 mm and the acceleration component "y" for the mold widths 1600 mm. This result is assumed because of the flow pattern differences, caused by the mold geometry.

It is relevant to visualize that for the mold width 900 mm the interface perturbation is higher than the observed for 1600 mm (for all the casting speeds, the acceleration components "x" and "y") in the zone near the nozzle. However, for the mold of 1600 mm only the acceleration component "x" values affect the interface perturbance. Considering the zone near the mold wall, a small perturbation was also observed for both acceleration components, however the entrapment susceptibility predicted at the interface near the wall is very low for the process conditions analyzed.

V. CONCLUSIONS

The computational simulation represents a very useful tool to obtain information about the fluid dynamic phenomena present in the continuous casting process, which are otherwise complex to study. The methodology applied shows high accuracy and reliable efficiency to evaluate the mold flux entrapment problem and could be used to predict casting product defects or to evaluate the impact of different mold fluxes or process variable changes in the industry. Due to the entrapment of the mold flux constitutes an important HSLA slab quality defect, which presents difficulties to be predicted under operation conditions selected for the study. This methodology provided the opportunity to evaluate and obtain information associated with different variables of CC process, decreasing the quality defects risk.

The simulation results determined that the HSLA steel product could avoid the mold powder entrapment risk for the mold widths (900 mm and 1600 mm) and with the mold flux selected, when the casting speed is 1 m/min and considering a SEN immersion depth of 100 mm. However, at higher casting speeds (1.5 m/min or 1.8 m/min) for the same SEN immersion depth (100 mm) the mold flux entrapment could be produced. The results showed that the casting speed 1.8 m/min constitutes the most critic for the casting system analyzed (with mold flux selected and HSLA steel). That is, the higher the speed casting is, the higher the entrapment susceptibility is. Probably for the critic casting speed conditions other mold flux could be selected to avoid product quality defect risks.

In addition, the results obtained show that the acceleration components values (x and y) allow to provide information of localized surface sites for the mold flux entrapment for each mold geometry and casting speeds, corroborating that the flow pattern induces the mold flux movement towards the wall of the SEN, probably stimulated by the hydrodynamic patterns which occurs in the immediate vicinity of the refractory piece.

The thermodynamics predictions carried out by the software Fact Sage 8.1, provide useful information of the steel and the mold flux at the process temperature conditions of interests. The results are used as input values in the fluid dynamic simulations and to predict physical properties behaviour of the mold flux for casting process of the HSLA steel.

ACKNOWLEDGMENT

The Authors are grateful for the financial support provided for the research to the Universidad Tecnológica Nacional from Argentina.

International Journal of Engineering Research & Technology (IJERT)
ISSN: 2278-0181
Vol. 12 Issue 02, February-2023

REFERENCES

[1] Z. Liu, B. Li,"Effect of vertical length on asymetric flow and inclusion transport in vertical bending continuous caster," Powder Technology, vol. 323, pp. 403-415, January 2018.

[2] K.C. Mills, C. Å Däcker, Using Mould Fluxes to Minimize Defects and Process Problems, 1st ed., vol 1. Springer, 2017. pp. 417-536.

[3] E. Brandaleze, G. Di Gresia, L. Santini, A. Martin and E. Benavidez, Mould Fluxes in the Steel Continuous Casting Process, 1st ed., vol.1. In Tech, 2012. pp.201-233.

[4] B.G. Thomas, "Modeling of the Coninuous Casting of Steel-Past, Present and Future," Electric Furnace Conference Proc. ISS, vol. 59, pp. 271-350, March 2002.

[5] Z. Liu, B. Li, L.Zhang, G. Xu, "Analysis of Transient Transport and Entrapment of Particle in Continuous casting Mold," ISIJ International, vol. 54, 10, pp. 2324-2333, June 2014.

[6] W.R.Irving, Continuous casting of steel, The Institute of Materials, , 1st ed., vol.1. In The University Press, Candbridge, 1983. pp. 93-155.

[7] M. Ślęzak, M. Warzecha, "Investigation of Liquid Steel Viscosity and Its Impact as the Initial Parameter on Modeling of the Steel Flow through the Tundish," Materials, vol. 13, 5025, pp.1-20, November 2020.

[8] K.C. Mills, A.B. Fox, R.P. Thackray and Z. Li, "The performance and properties of mould fluxes," VII International Conference on Molten Slags Fluxes and Salts," The South African Institute of Mining and Metallurgy, pp. 713-722, Agoust 2004.

[9] E. Brandaleze, M. Valentini, L. Santini, E. Benavidez, "Study on fluoride evaporation from casting powders," Journal of Thermal Analysis and Calorimetry, vol. 133, pp. 271-277, April 2018.

[10] T. Witelski, M. Bowen, Method of Mathematical Modelin- Continuous Systems and Differential Equations, 1st ed., vol.1. In Springer, 2015.

[11] R. Kaushik, M.K. Srivastava, "Investigation of 2-Dimensional Fluid Flow using Finite Difference Flow Method of Navier Stokes Equation," International Journal of Engineering Research & Technology (IJERT), vol. 11, 2, pp. 127- 132, February-2022.

[12] A. Cwudziński, J. Jowsa, P. Przegrałek, "Interaction of liquid steel with mould flux in continuous casting bloom mould-numerical simulations and industrial experiences," Arch. Metall. Mater., vol. 61, 4, pp. 2013-2020, December 2016.

[13] M.Flaman, E. Brandaleze, "Impact of casting process conditions on the structure and ductility of an AHSS steel slab," Journal of Multidisciplinary Engineering Science and Technology, vol. 6, 1, pp. 9328-9335, January 2019.

[14] J. Yang, D. Chen, M. Long, H. Duan, "Transient flow and mold flux behaviour during ultra-high speed continuous casting of billet," Journal of Materials Research and Technology, vol. 9, 3, pp. 3984-3993, June 2020.

[15] X. Zhang, W. Zhang, J. Jin, J.W. Evans, "Flow of Steel in Mold Region During Continuous Casting," Journal of Iron and Steel Research International, vol. 14, 2, pp. 30-35. February 2007.

[16] W. Zhang, J. Gao, P.K. Rohatgi,H. Zhao, Y. Li, "Effect of the depth of the submerged entry nozzle in the mold on heat, flow and solution transport in double-stream-pouring continuous casting," Journal of Materials Processing Technology, vol. 209, pp. 5536–5544, April 2009.